Supplement of The Cryosphere, 17, 4007–4020, 2023
https://doi.org/10.5194/tc-17-4007-2023-supplement

The Cryosphere Open Access EGU

Supplement of

Early Holocene ice on the Begguya plateau (Mt. Hunter, Alaska) revealed by ice core ^{14}C age constraints

Ling Fang et al.

Correspondence to: Theo M. Jenk (theo.jenk@psi.ch)

Supplementary

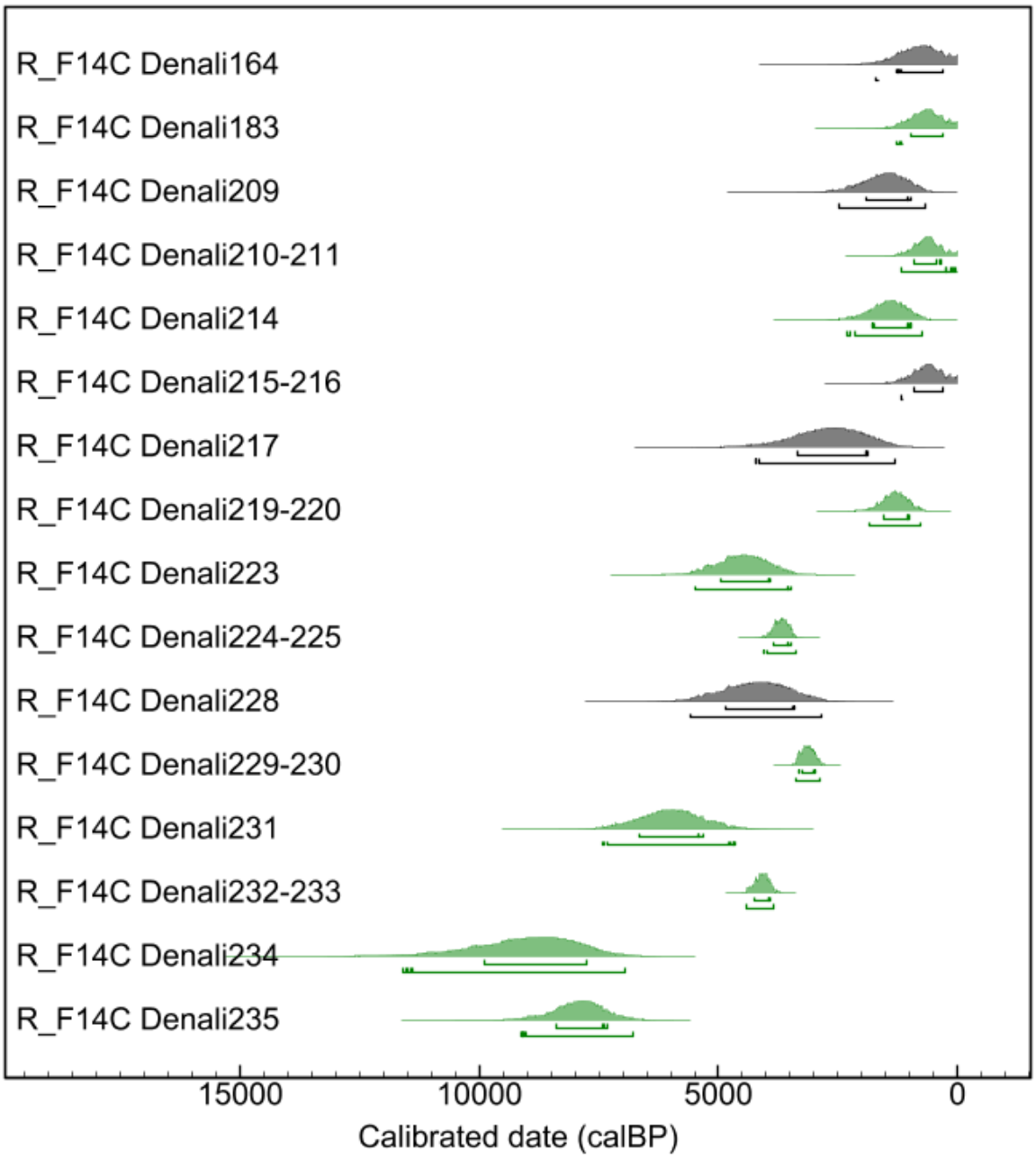

Figure S1 Calibrated ^{14}C ages for all Denali ice core samples as derived in OxCal v4.4.4 using the Northen Hemispheric IntCal20 radiocarbon calibration curve (Ramsey 2021; Reimer et al. 2020). Here, without applying the sequence model (no constraint by assuming sequential ordering of samples). Shown are probability distributions of calibrated dates for samples significantly >10 µg C (green) and <10 µg C (grey) for AMS analysis. 1σ and 2σ ranges of the calibrated ages are indicated by the respective lines below.

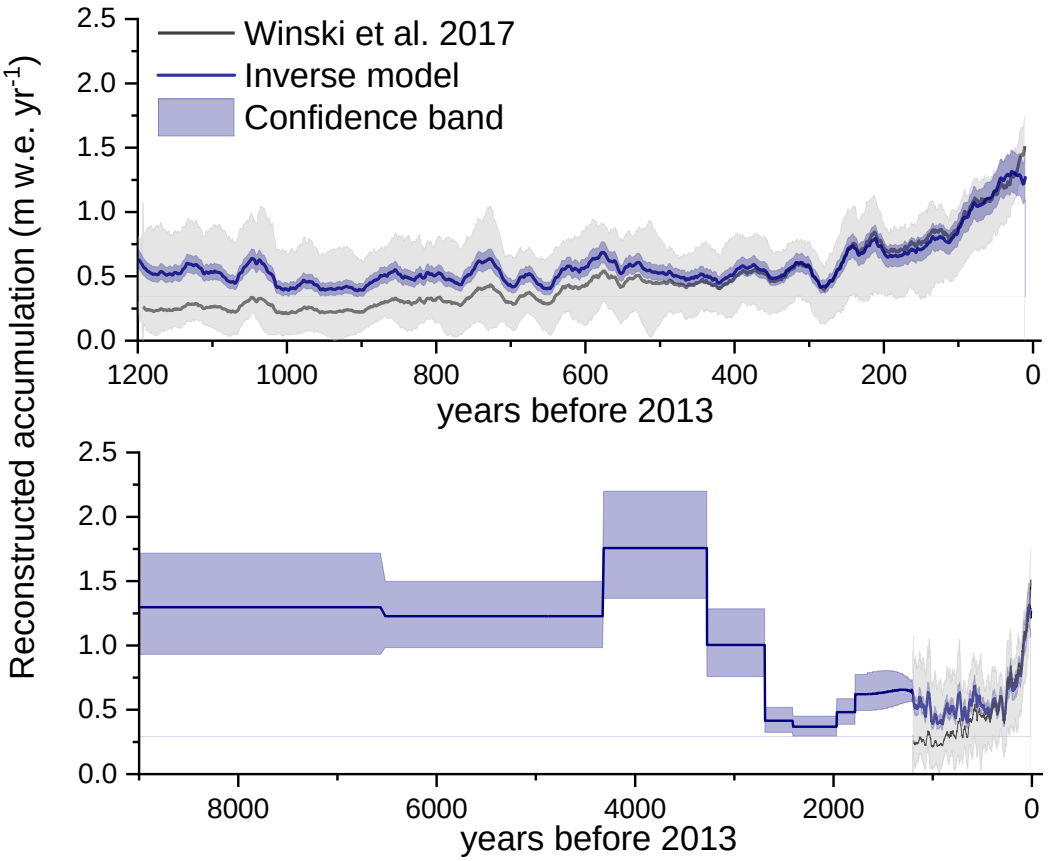

Figure S2 Upper panel: Reconstructed annual net accumulation rates from the inverse model (navy line and shading) compared with reported values, based on a 3D model, from Winski et al. 2017 (black line and shading). Lower panel: Reconstructed accumulation from this study, extended back in time.

Table S1 ^{14}C results of all Denali ice core samples, here with calibrated ages (OxCal v4.4.4, IntCal20) as derived if the sequence model is not applied, and also for samples < 10 µg C (see main text).

Sample ID	AMS Lab ID	Depth (m)	Mid Depth (m w.e.)	Carbon amount (µg C)	WIOC (µg kg^{-1})	$F^{14}C$ (1σ)	Calibrated ^{14}C age (cal BP, 1σ range)
Denali164*	BE-10013.1.1	148.6-149.4	115.90	7	6.2	0.910 ± 0.058	306-1260
Denali183	BE-10015.1.1	165.7-166.6	131.40	11	10.1	0.921 ± 0.042	299-971
Denali209*	BE-10016.1.1	187.8-188.7	151.16	9	9.8	0.826 ± 0.044	977-1925
Denali210-211	BE-8997.1.1	188.7-190.3	152.29	11	20.0	0.922 ± 0.033	327-918
Denali214	BE-10017.1.1	192.1-192.9	155.00	14	11.8	0.831 ± 0.036	979-1775
Denali215-216*	BE-8998.1.1	193.0-194.7	156.17	9	12.0	0.925 ± 0.039	305-924
Denali217*	BE-10018.1.1	194.7-195.5	157.33	7	6.1	0.731 ± 0.054	1890-3351
Denali219-220	BE-8615.1.1	196.4-197.3	159.31	12	16.8	0.841 ± 0.026	1001-1539
Denali223	BE-10019.1.1	199.8-200.7	161.93	21	17.3	0.608 ± 0.029	3922-4966
Denali224-225	BE-11923.1.1	200.7-202.3	163.06	34	17.5	0.653 ± 0.010	3494-3835
Denali228*	BE-10020.1.1	203.5-204.2	165.11	9	10.0	0.627 ± 0.043	3415-4861
Denali229-230	BE-11924.1.1	204.2-205.7	166.09	39	20.0	0.691 ± 0.009	2972-3326
Denali231	BE-10021.1.1	205.7-206.6	167.18	11	11.5	0.523 ± 0.037	5321-6656
Denali232-233	BE-11925.1.1	206.6-208.1	168.26	55	30.8	0.629 ± 0.008	3922-4237
Denali234	BE-10022.1.1	208.1-208.8	169.23	10	11.7	0.378 ± 0.043	7740-9894
Denali235#	BE-12465.1.1	208.8-209.4	169.83	21	80.3_{DOC}	(0.437 ± 0.025)	(7043-7999)
						0.418 ± 0.027$	7334-8404$

*Carbon mass < 10 µg C (excluded for final dating, see main text).

#Results from the DOC fraction.

$After correction for in-situ ^{14}C (Fang et al. 2021; see main text)